

**DEVELOPMENT AND APPLICATIONS OF BENCHMARK EXAMPLES
FOR STATIC DELAMINATION PROPAGATION PREDICTIONS**

Ronald Krueger

National Institute of Aerospace
NASA Langley Research Center, Hampton, VA, USA

*Paper submitted to the 28th Annual Technical Conference of the
American Society for Composites*

ABSTRACT

The development and application of benchmark examples for the assessment of quasi-static delamination propagation capabilities was demonstrated for ANSYS[®] and Abaqus/Standard[®]. The examples selected were based on finite element models of Double Cantilever Beam (DCB) and Mixed-Mode Bending (MMB) specimens. First, quasi-static benchmark results were created based on an approach developed previously. Second, the delamination was allowed to propagate under quasi-static loading from its initial location using the automated procedure implemented in ANSYS[®] and Abaqus/Standard[®]. Input control parameters were varied to study the effect on the computed delamination propagation. Overall, the benchmarking procedure proved valuable by highlighting the issues associated with choosing the appropriate input parameters for the VCCT implementations in ANSYS[®] and Abaqus/Standard[®]. However, further assessment for mixed-mode delamination fatigue onset and growth is required. Additionally studies should include the assessment of the propagation capabilities in more complex specimens and on a structural level.

INTRODUCTION

Over the past two decades, the use of fracture mechanics has become common practice to characterize the onset and growth of delaminations. In order to predict delamination onset or growth, the calculated strain energy release rate components are compared to interlaminar fracture toughness properties measured over a range from pure mode I loading to pure mode II loading.

*R. Krueger, National Institute of Aerospace, 100 Exploration Way, Hampton, VA, 23666.
This work was performed at the Durability, Damage Tolerance and Reliability Branch, MS 188E, NASA Langley Research Center, Hampton, VA, 23681, USA.

The virtual crack closure technique (VCCT) is widely used for computing energy release rates based on results from continuum (2D) and solid (3D) finite element (FE) analyses and to supply the mode separation required when using the mixed-mode fracture criterion [1, 2]. The virtual crack closure technique was recently implemented into several commercial finite element codes such as Abaqus/Standard[®], MD Nastran[™], Marc[™] and ANSYS[®]. As new methods for analyzing composite delamination are incorporated into finite element codes, the need for comparison and benchmarking becomes important since each code requires specific input parameters unique to its implementation. These parameters are unique to the numerical approach chosen and do not reflect real *physical* differences in delamination behavior.

An approach for assessing the mode I, and mixed-mode I and II, delamination propagation capabilities in commercial finite element codes under static loading was recently presented and demonstrated for the VCCT implementation in Abaqus/Standard[®] [3-5] as well as MD Nastran[™] and Marc[™] [6] and ANSYS[®] [7]. First, benchmark results were created manually for finite element models of the mode I Double Cantilever Beam (DCB), the mode II End Notched Flexure (ENF) as well as the mixed-mode I/II Single Leg Bending (SLB) and Mixed-Mode Bending (MMB) specimens. Second, the delamination was allowed to propagate under quasi-static loading from its initial location using the automated procedure implemented in the finite element software. The approach was then extended to allow the assessment of the delamination fatigue growth prediction capabilities in commercial finite element codes [4, 8]. As for the static case, benchmark results were created manually first for the mode I Double Cantilever Beam (DCB) and the mode II End Notched Flexure (ENF) specimen. Second, the delamination was allowed to grow under cyclic loading in a finite element model of a commercial code. For all cases, input control parameters were varied to study the effect on the computed delamination propagation and growth. The benchmarking procedure proved valuable by highlighting the issues associated with choosing the input parameters of the particular implementation. Consequently, the benchmark enabled the selection of the appropriate input parameters that yielded good agreement between the results obtained from the growth analysis and the benchmark results. Once the parameters have been identified, they may then be used with greater confidence to model delamination growth for more complex configurations.

In this paper, the benchmark analysis from previous studies is summarized using the Double Cantilever Beam (DCB) and the Mixed-Mode Bending (MMB) specimens as examples [3, 5, 7]. Special attention is given first to the creation of the benchmark case, which is independent of the analysis software. The benchmark case allows the assessment of the automated delamination propagation prediction capabilities in commercial finite element codes based on the virtual crack closure technique (VCCT). Examples of automated propagation analyses are then shown for two different finite element codes (Abaqus/Standard[®] and ANSYS[®]) and the selection of the required code specific input parameters is discussed. Examples using MD Nastran[™] and Marc[™] are discussed in reference 6.

SPECIMEN CONFIGURATIONS SELECTED AS BENCHMARK CASES

For the current summary, two simple specimens used for fracture toughness testing were selected. These specimens had been used previously to develop the current approach for assessment of the quasi-static delamination propagation simulation capabilities in commercial finite element codes [3-7]. The Double Cantilever Beam (DCB) specimen, as shown in Figure 1, was chosen since it only exhibits the mode I opening fracture mode. Besides the previously developed benchmark case of the DCB specimen [3], an additional example was used for which experimental data also exist for comparison. This example was published by *NAFEMS* - an independent not-for-profit body with the sole aim of promoting the effective use of engineering simulation methods - as part of their benchmark cases [9].

One example that exhibits mixed-mode I/II fracture was also selected: The Mixed-Mode Bending (MMB) specimen, as shown in Figure 2, was studied for 80% mode II [5,7]. The material and overall specimen dimensions including initial crack length, a_0 , are shown in the respective figures. All configurations had layups of $[0]_{24}$. The material properties are given in references 3, 5 and 7. A methodology for delamination propagation, onset and growth based on fracture mechanics [10] was used to create the benchmark examples.

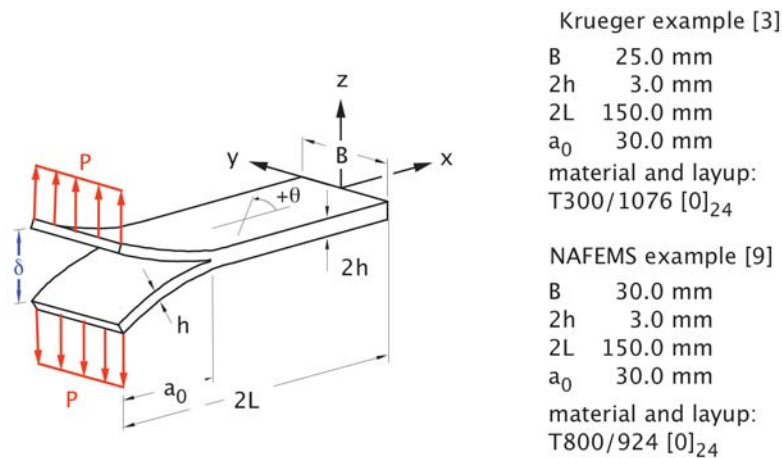


Figure 1. Double Cantilever Beam specimen (DCB): Dimensions and Layup [3,7].

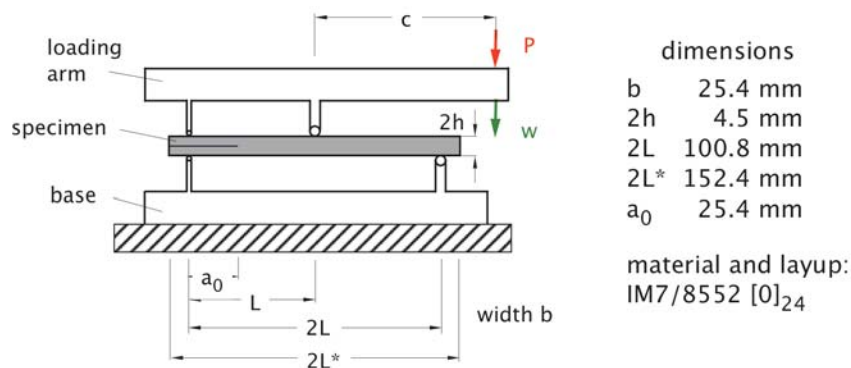


Figure 2. Mixed-Mode Bending specimen (MMB): Dimensions and Layup [5,7].

METHODOLOGY BASED ON FRACTURE MECHANICS

A quasi-static mixed-mode fracture criterion is discussed first, since the parameters are required input to the VCCT implementation in Abaqus/Standard[®] and ANSYS[®]. The input details of the specific codes are discussed in references 3 and 7. The mixed-mode fracture criterion for a material is determined by plotting the interlaminar fracture toughness, G_c , versus the mixed-mode ratio, G_{II}/G_T , as shown in Figure 3 for a typical carbon/epoxy material. The fracture criterion is generated experimentally using pure Mode I ($G_{II}/G_T=0$) Double Cantilever Beam (DCB) tests (as shown in Figure 1), pure Mode II ($G_{II}/G_T=1$) End-Notched Flexure (ENF) tests, and Mixed Mode Bending (MMB) tests (as shown in Figure 2), of varying ratios of G_{II}/G_T . The mean values (filled blue circles) are shown in Figure 3. A 2D fracture criterion was suggested by Benzeggah and Kenane [11] using a simple mathematical relationship between G_c and G_{II}/G_T

$$G_c = G_{Ic} + (G_{IIc} - G_{Ic}) \left(\frac{G_{II}}{G_T} \right)^\eta \quad (1)$$

In this expression, typically called the B-K criterion, G_{Ic} and G_{IIc} are the experimentally determined fracture toughness data for mode I and II as shown in Figure 3. The exponent η was determined by a curve fit. The parameters G_{Ic} , G_{IIc} and η are required input to perform a VCCT analysis in Abaqus/Standard[®] [12] and ANSYS[®] [13, 14]. Example input is provided in references 3, 5 and 7.

During an automated propagation analysis, the total strain energy release rate, G_T , and the mixed-mode ratio G_{II}/G_T are computed using VCCT. The failure index, G_T/G_c , is calculated by correlating the computed total energy release rate, G_T , with the mixed-mode fracture toughness, G_c , of the graphite/epoxy material. As shown in equation (1) the mixed-mode fracture toughness, G_c , is a function of the mixed-mode ratio G_{II}/G_T (see also Figure 3). An example how to obtain G_c for $G_{II}/G_T=0.8$ has been included in Figure 3 (purple arrows). It is assumed that the delamination propagates when the failure index, G_T/G_c , reaches unity.

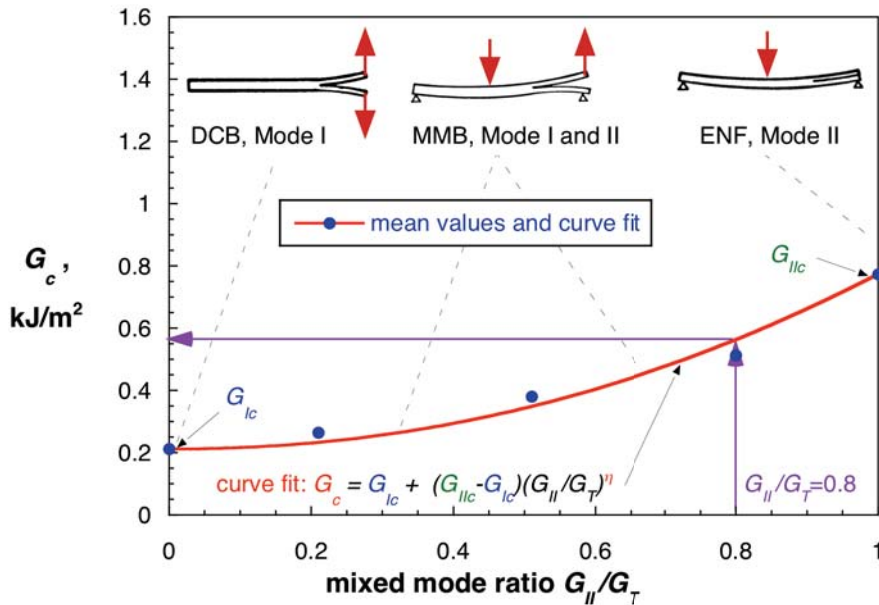


Figure 3. Mixed mode fracture criterion for a typical carbon/epoxy material.

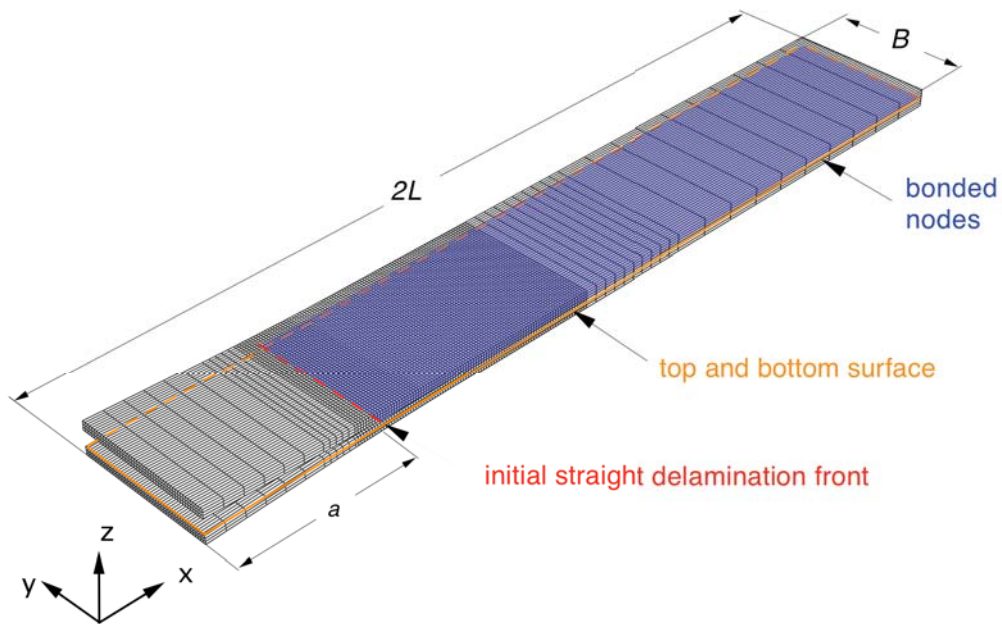
FINITE ELEMENT MODELING

Model description

Finite element models of the specimens are shown in Figures 4 and 5. For two-dimensional (2D) analyses the specimens were modeled with plane strain elements such as *CPE4I* in Abaqus/Standard® [12] and *PLANE182* in ANSYS® [13-14]. Three-dimensional (3D) analyses were only performed using Abaqus/Standard® and solid brick elements *C3D8I* were used to model the specimens. Along the length, all models were divided into different sections with different mesh refinement as shown in Figures 4 and 5. A typical finite element model of a DCB specimen is shown in Figure 4. The DCB specimen was modeled with six elements through the specimen thickness ($2h$). The resulting element length at the delamination tip was $\Delta a=0.5$ mm.



(a). Deformed model of a DCB specimen (plane strain *CPE4* elements in Abaqus/Standard® and *PLANE182* elements in ANSYS®) [7,8].



(b). Three-dimensional model (solid *C3D8I* elements in Abaqus/Standard®)[3].

Figure 4. Double Cantilever Beam specimen (DCB).

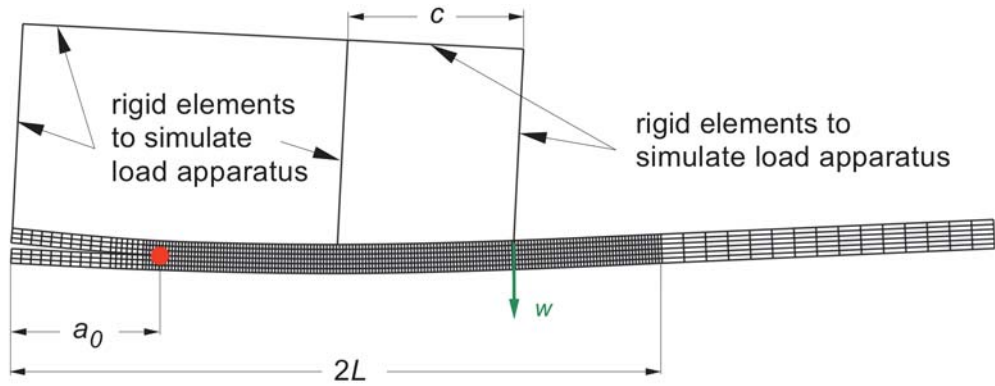


Figure 5. Two-dimensional model (plane strain CPE4I elements in Abaqus/Standard[®]) of a MMB specimen [5,7].

A two-dimensional finite element model of a MMB specimen with boundary conditions is shown in Figure 5. Along the length, all models were divided into different sections with different mesh refinement as discussed earlier. The MMB specimen was also modeled with six elements through the specimen thickness. The resulting element length at the delamination tip was $\Delta a = 0.5$ mm. The load apparatus was modeled explicitly using rigid beam elements (R2D2) as shown in Figure 5. Multi-point constraints were used to connect the rigid elements with the solid model of the specimen and enforce the appropriate boundary conditions. The mixed-mode ratio G_{II}/G_T is controlled by the length, c , of the loading arm. Configurations were developed that yielded mode ratios of 20% mode II ($G_{II}/G_T = 0.2$), 50% mode II ($G_{II}/G_T = 0.5$), and 80% mode II ($G_{II}/G_T = 0.8$) [5,7]. Here, only the model for 80% mode II is shown for which results will be presented later.

For all models, the plane of delamination was modeled as a discrete discontinuity in the center of the specimen. The models were created as separate meshes for the upper and lower part of the specimens with identical nodal point coordinates in the plane of delamination and contact was used to define the intact section of the specimen. Details of the modeling are discussed in references 3, 5 and 7.

Quasi-static delamination propagation analysis

For the automated delamination propagation analysis, the VCCT implementation in Abaqus/Standard[®] 6.10 [12] and in ANSYS[®] 13.0 beta and 14.0 beta were used [13, 14]. It is implied that the energy release rate at the crack tip is calculated at the end of a converged increment. Once the energy release rate exceeds the critical strain energy release rate (including the user-specified mixed-mode criteria as shown in Figure 3), the node at the crack tip is released in the following increment, which allows the crack to propagate. For automated propagation analysis, it was assumed that the computed behavior should closely match the benchmark results created below. For all analyses, the elastic constants and the input to define the fracture criterion were kept constant. Only code specific,

implementation dependent parameters were varied to improve convergence and achieve better results.

In addition to the mixed-mode fracture criterion, Abaqus/Standard[®] requires extra input for the propagation analysis. If a user specified release tolerance is exceeded in an increment $(G-G_c)/G_c > \text{release tolerance}$, a cutback operation is performed which reduces the time increment. In the new smaller increment, the strain energy release rates are recalculated and compared to the user specified release tolerance. The cutback reduces the degree of overshoot and improves the accuracy of the local solution [12]. A release tolerance of 0.2 is suggested in the handbook [12]. Further, to help overcome convergence issues during the propagation analysis, Abaqus/Standard[®] provides:

- *contact stabilization* which is applied across only selected contact pairs and used to control the motion of two contact pairs while they approach each other in multi-body contact. The damping is applied when bonded contact pairs debond and move away from each other [12]
- *automatic or static stabilization* which is applied to the motion of the entire model and is commonly used in models that exhibit statically unstable behavior such as buckling [12]
- *viscous regularization*, which is applied only to nodes on contact pairs that have just debonded. The viscous regularization damping causes the tangent stiffness matrix of the softening material to be positive for sufficiently small time increments. Viscous regularization damping in Abaqus/Standard[®] is similar to the viscous regularization damping provided for cohesive elements and the concrete material model in Abaqus/Standard[®] [12]. Further details about the required input parameters are discussed in references 5 and 7.

The VCCT implementation in ANSYS[®] does not require the user to specify a release tolerance. Also stabilization criteria to help overcome convergence issues were not available in the ANSYS[®] releases studied. The following specific input parameters could be altered by the user in order to achieve better results during an automated delamination propagation analysis:

- The initial time step size and maximum step size for crack growth (*cgrow*) were varied. The parameters are called *dtime* and *dtmax*.
- The automated time stepping (*autots*) was also studied in detail. The input parameters, which were varied are also called *dtime* and *dtmax*³. Further details about the required input parameters are discussed in reference 9.

PROCEDURE FOR DEVELOPING QUASI-STATIC BENCHMARK CASES

Based on the approach developed earlier [3], quasi-static benchmark results can be created for any analysis software used. The procedure is outlined using the DCB specimen with a unidirectional layup (as shown in Figure 1) as an example. This specimen configuration was chosen as a benchmark case for mode I, since it is

³ Note that the input parameters for both crack growth time step (*cgrow*) and automated time stepping (*autots*) are called *dtime* and *dtmax*. For more clarity *dtimea* and *dtmaxa* were used for the parameters for automated time stepping (*autots*).

simple and a number of numerical studies had been performed previously to evaluate the critical strain energy release rates. To avoid unnecessary complications, experimental anomalies such as fiber bridging were not addressed [3].

- First, finite element models of the specimen with different delamination lengths, a_0 , have to be created. For the current example two-dimensional finite element models simulating the DCB specimens with 17 different delamination lengths a_0 were created ($30.5 \text{ mm} \leq a_0 \leq 69.5 \text{ mm}$).
- For each delamination length, a_0 , modeled, the load, P , and opening displacement, $\delta/2$, at the load point were plotted as shown in Figure 6 (dashed colored and solid grey lines)
- For each delamination length, a_0 , modeled, the mixed-mode strain energy release rate components were computed using VCCT for applied displacements $\delta/2 = 1.5 \text{ mm}$ (for $a_0 < 45.4 \text{ mm}$), and $\delta/2 = 3 \text{ mm}$ (for $45.4 \text{ mm} \leq a_0 < 65.4 \text{ mm}$) and $\delta/2 = 5 \text{ mm}$ (for $65.4 \text{ mm} \leq a_0 \leq 69.5 \text{ mm}$). The total energy release rate is a function of the delamination length, a_0 , and the applied opening displacement, $\delta/2$, as indicated in Figure 6, thus $G_T = G_T(a_0, \delta/2)$. For the simple case of the mode I DCB specimen shown, the computed values were predominantly mode I as expected.
- For each delamination length, a_0 , modeled, a failure index, G_T/G_c , is calculated by correlating the computed total energy release rate, G_T , with the mixed-mode fracture toughness, G_c , of the material shown in Figure 3. For the simple case of the DCB specimen shown, the failure index is simply calculated as G_I/G_{Ic} . It is assumed that the delamination propagates when the failure index reaches unity.
- Therefore, the critical load, P_{crit} , and critical opening displacement, $\delta_{crit}/2$ can be calculated - for each delamination length, a_0 , modeled - based on the relationship between load, P , and the energy release rate, G [15],

$$G = \frac{P^2}{2} \cdot \frac{\partial C_P}{\partial A} \quad (2)$$

In equation (2), C_P is the compliance of the specimen, and ∂A is the increase in surface area corresponding to an incremental increase in load or displacement at fracture. The critical load, P_{crit} , and critical opening displacement, $\delta_{crit}/2$ can be calculated for each delamination length, a_0 , modeled

$$\frac{G_T}{G_c} = \frac{P^2}{P_{crit}^2} \Rightarrow P_{crit} = P \sqrt{\frac{G_c}{G_T}}; \text{ and } \frac{\delta_{crit}}{2} = \frac{\delta}{2} \sqrt{\frac{G_c}{G_T}} \quad (3)$$

and the results can be included in the load/displacement plots as shown in Figure 7 (solid red circles).

- By fitting a curve through these critical load/displacement results (solid red circles), a benchmark solution (thick solid red line) can be created as shown in Figure 7.

During the automated propagation analysis, the computed load/displacements results are expected to follow the benchmark solution.

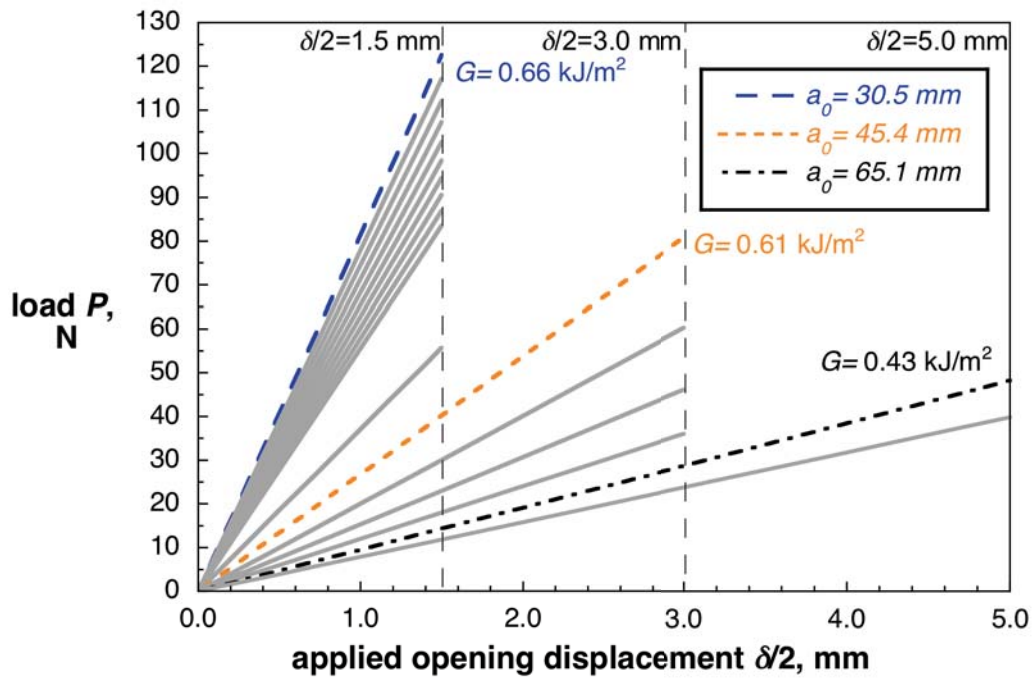


Figure 6. Computed load-displacement behavior of a DCB specimen for different delamination lengths a_0 .

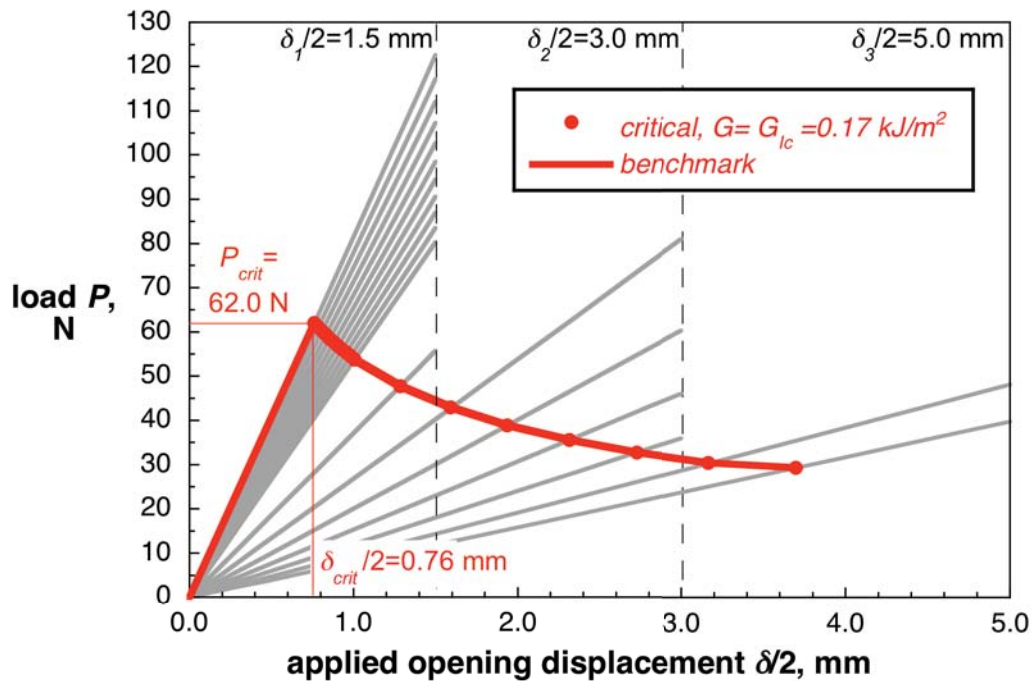


Figure 7. Calculated critical behavior and resulting benchmark case for a DCB specimen.

QUASI-STATIC ANALYSIS BENCHMARKING

Quasi-Static Benchmark Case for Mode I

Automated delamination propagation analysis using Abaqus/Standard®

A set of example results using Abaqus/Standard® are shown in Figure 8 where the computed resultant force (load P) at the tip of the DCB specimen is plotted versus the applied crack tip opening ($\delta/2$) for different input parameters [3]. To overcome the convergence problems, the methods implemented in Abaqus/Standard® were used independently to study the effects [12]. First, global stabilization was used in the analysis. For a stabilization factor of 2×10^{-5} , the stiffness changed to almost infinity once the critical load was reached causing the load to increase sharply (thick solid red). The load increased until a point was reached where the delamination propagation started and the load gradually decreased following a saw tooth curve with local rising and declining segments. The gradual load decrease followed the same trend as the benchmark curve (solid grey line) but is shifted toward higher loads. For a stabilization factor of 2×10^{-6} (solid green line), the same saw tooth pattern was observed but the average curve was in good agreement with the benchmark result. Second, contact stabilization was used in the analysis. For all combinations of stabilization factors and release tolerances, a saw tooth pattern was observed, where the peak values were in good agreement with the benchmark result (solid blue line). Third, the use of viscous regularization to overcome convergence problems was studied. Convergence could not be achieved over a wide range of viscosity coefficients when a default release tolerance value of 0.2 was used.

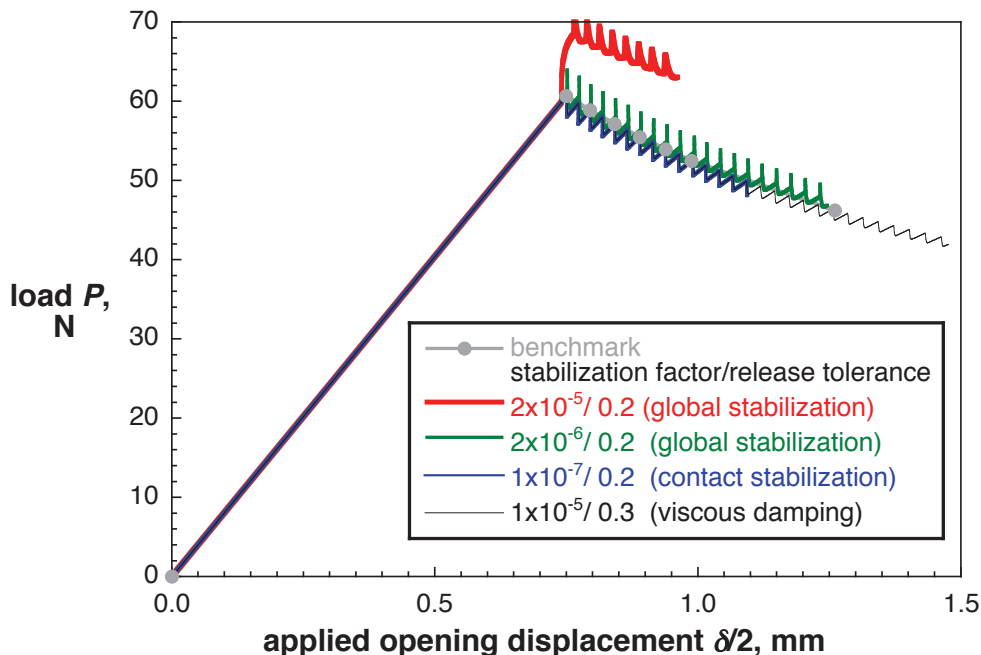


Figure 8. Computed critical load-displacement behavior for a DCB specimen obtained from 3D solid models (C3D8I).

Subsequently, the release tolerance value was increased. For all combinations of the viscosity coefficient and release tolerance, where convergence was achieved, a saw tooth pattern was obtained, where the peak values were in good agreement with the benchmark result (thin solid black line).

The examples shown highlight the importance of benchmarking to identify critical analysis input parameters. In summary, good agreement between the load-displacement relationship obtained from the propagation analysis results and the benchmark results could be achieved by selecting the appropriate input parameters. However, selecting the appropriate VCCT input parameters such as release tolerance, global or contact stabilization and viscous regularization, was not straightforward and often required an iterative procedure. The default setting for global stabilization yielded unsatisfactory results although the analysis converged. Detailed results for Abaqus/Standard[®] are discussed in reference 3.

Automated delamination propagation analysis using ANSYS[®]

The automated propagation analysis in ANSYS[®] was performed in one step. Starting from an initial delamination length, $a_0=30.5$ mm, the delamination was allowed to propagate based on the algorithms implemented into ANSYS[®] [7]. A total crack opening displacement $\delta/2=2.0$ mm was applied to each cantilever arm. Results from the first set of propagation analyses are shown in Figure 9.

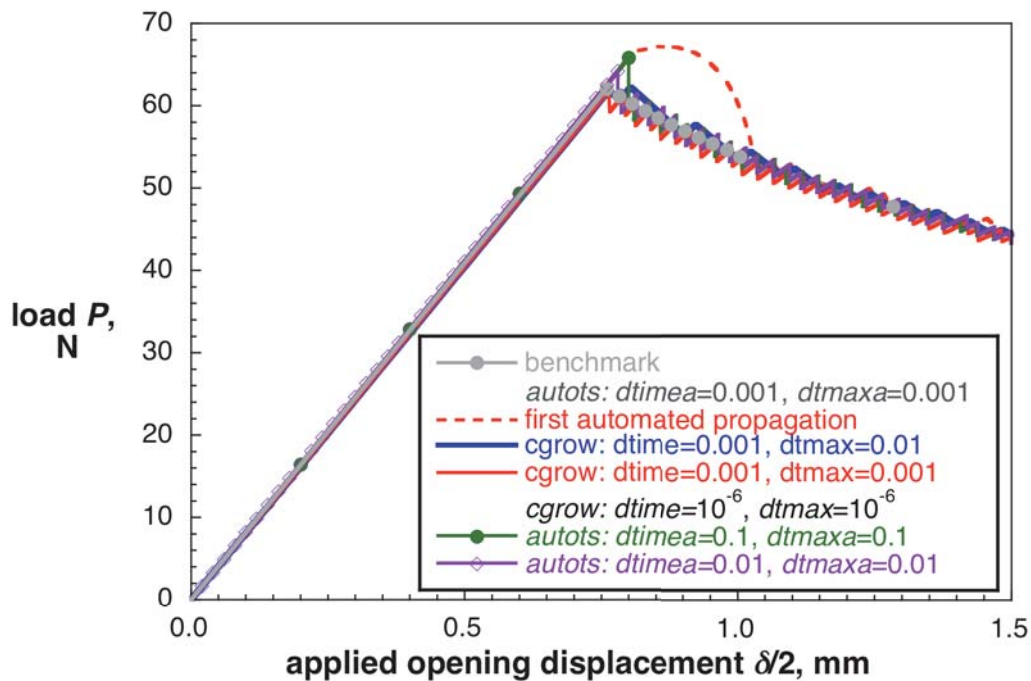


Figure 9. Computed critical load-displacement behavior for a DCB specimen obtained from 2D planar models (PLANE182).

For the first propagation analysis (dashed red line), the stiffness of the specimen remained unchanged once the critical point was reached and load and displacement kept increasing. Later, the stiffness decreased as the delamination propagated, the load started to drop and the computed load/displacement path converged to the benchmark result (solid grey circles and solid grey line). In order to minimize the undesirable overshoot and to closely capture the critical point, the parameters ($dtime$ and $dtmax$) had to be specified to control the time step for crack growth ($cgrow$). For an initial time step, $dtime=0.001$, and maximum allowable time step, $dtmax=0.01$ - so that the analysis could adjust the parameter as needed - the result (solid blue line) was in good agreement with the benchmark result. Improved results (solid red line) could be obtained when the maximum allowable time step was limited to $dtmax=0.001$

Additionally, the effect on the computed results caused by the input parameters ($dtimea$ and $dtmaxa$) for automated time stepping ($autots$) was studied. The effect was studied in more detail while – based on the study from above - the input to control the time step for crack growth was kept constant ($dtime=dtmax=10^{-6}$). For automated time steps $dtimea=dtmaxa=0.1$ ($dtmina=10^{-6}$), the results (solid green line) overshoot the critical point as shown in Figure 9. Once delamination propagation started, the load instantly dropped and the analysis continued to follow the benchmark (solid grey circles and solid grey line). For $dtimea=dtmaxa=0.01$, the overshoot was less pronounced (solid purple line). It appears that crack propagation starts at the time step after which the critical point has been exceeded for the first time. As shown in the plots, this time step depends on the step size (green dots and purple diamonds). There is no apparent automated cut back procedure that forces a reanalysis of the last step with a smaller time step, which would allow the analysis to zero in on the critical point. The implementation of a user defined release tolerance, which triggers a cut back might alleviate this observed problem.

In summary, input parameters for automated time stepping ($autots$) need to be chosen by the user such that the time steps are sufficiently small to capture the critical point for propagation onset (first node release) correctly. The input parameters, which control the time step for crack growth however, appear to have an effect only on the quality of results during propagation. The results suggest that small time steps are required to obtain accurate results. However, such small steps cause an increase in computation time as discussed later. Long computation times, however, may be avoided by splitting the analysis in two parts. During the first part, the analysis remains subcritical and the delamination does not propagate so that large time steps can be used for automated time stepping. The first part of the analysis is set to end just before the analysis reaches the critical point. During the second part of the analysis, the time steps for automated time stepping are reduced to accurately capture the critical point. Additionally, the time steps for crack growth are selected to be sufficiently small to assure a proper propagation analysis.

NAFEMS DCB benchmark case for mode I

To highlight the independence of the benchmark procedure from the analysis code used, another DCB specimen with slightly different dimensions and material properties (shown in Figure 1) was selected. For this configuration experimental as

well as analytical results were available. This example was published by *NAFEMS* as part of their benchmark examples [8]. The experiments exhibited only a negligible amount of fiber bridging so that comparison with the analysis appeared justified [8]. Following the same procedure outlined above, two benchmark results were created for ANSYS[®] and Abaqus/Standard[®] using the same model shown in Figure 4a. As shown in the plots of Figure 10, the computed benchmark results for ANSYS[®] (open red circles and solid red line) compared well with the benchmark results for Abaqus/Standard[®] (solid black diamond and solid black line) [3] as well as and the experimental data (solid blue squares) published in reference 8. The benchmark results also agree with the analytical results (thick dashed green line).

Quasi-Static Benchmark Cases for Mixed-Mode I/II

Development of benchmark cases for 80% mode II based on the MMB specimen

A benchmark case for 80% mode II ($G_{II}/G_T = 0.8$) was created based on the approach discussed above for mode I. Two-dimensional finite element models simulating MMB specimens with 15 different delamination lengths a_0 were created ($25.4 \text{ mm} \leq a_0 \leq 70.6 \text{ mm}$) to study the case of $G_{II}/G_T = 0.8$. An example of a finite element model is shown in Figure 5. For each delamination length modeled, the load, P , and displacement, w , were monitored as shown in Figure 11 (dashed colored and solid grey lines). Using VCCT, the total energy release rate, G_T , and the mixed-mode ratio G_{II}/G_T were computed at the end of the analysis as shown in Figure 11.

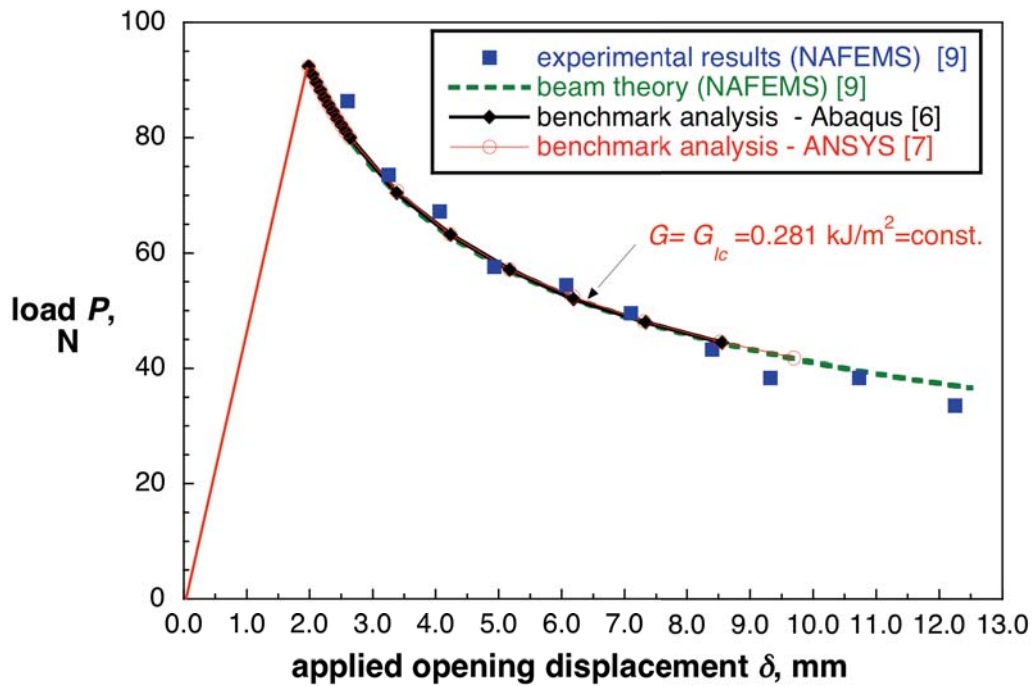


Figure 10. Benchmark case for NAFEMS DCB specimen.

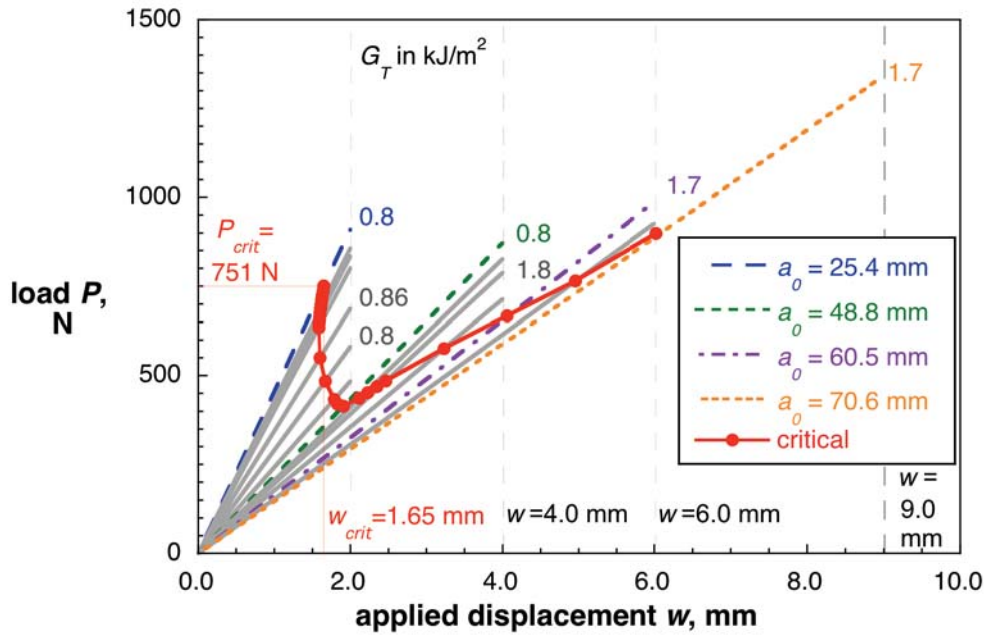


Figure 11. Calculated critical load-displacement behavior for a MMB specimen (80% mode II) obtained from 2D planar models (CPE4I).

The critical mixed-mode fracture toughness, G_c for each computed mixed-mode ratio ($G_{II}/G_T \approx 0.8$) was obtained from the curve fit of the material data (solid red curve) as illustrated in Figure 3 (purple arrows). The critical load, P_{crit} , and critical displacement, w_{crit} , were calculated for each delamination length modeled, using equation (3), and the results were included in the load/displacement plots as shown in Figure 11 (solid red circles).

These critical load/displacement results indicated that, with increasing delamination length, less load is required to extend the delamination. For the first five delamination lengths, a_0 , plotted in Figure 11, the values of the critical displacements also decreased at the same time. This means that the MMB specimen exhibits unstable delamination propagation under load control as well as displacement control in this region for $G_{II}/G_T = 0.8$. The remaining critical load/displacement results indicated stable propagation. From these critical load/displacement results (solid grey circles and dashed line), two benchmark solutions can be created as shown in Figure 12.

During the analysis, either prescribed displacements, w , or nodal point loads, P , are applied. For the case of prescribed displacements, w , (dashed blue line), the applied displacement must be held constant over several increments once the critical point (P_{crit} , w_{crit}) is reached, and the delamination front is advanced during these increments. Once the critical path (dashed grey line) is reached, the applied displacement is increased again incrementally. For the case of applied nodal point loads (dashed red line), the applied load must be held constant while the delamination front is advanced during these increments. Once the critical path (dashed grey line) is reached, the applied load is increased again incrementally. It is assumed that the load/displacement relationship computed during automatic propagation should closely match the benchmark case. Benchmark cases for 20% and 50% mode II are discussed in detail in reference 5.

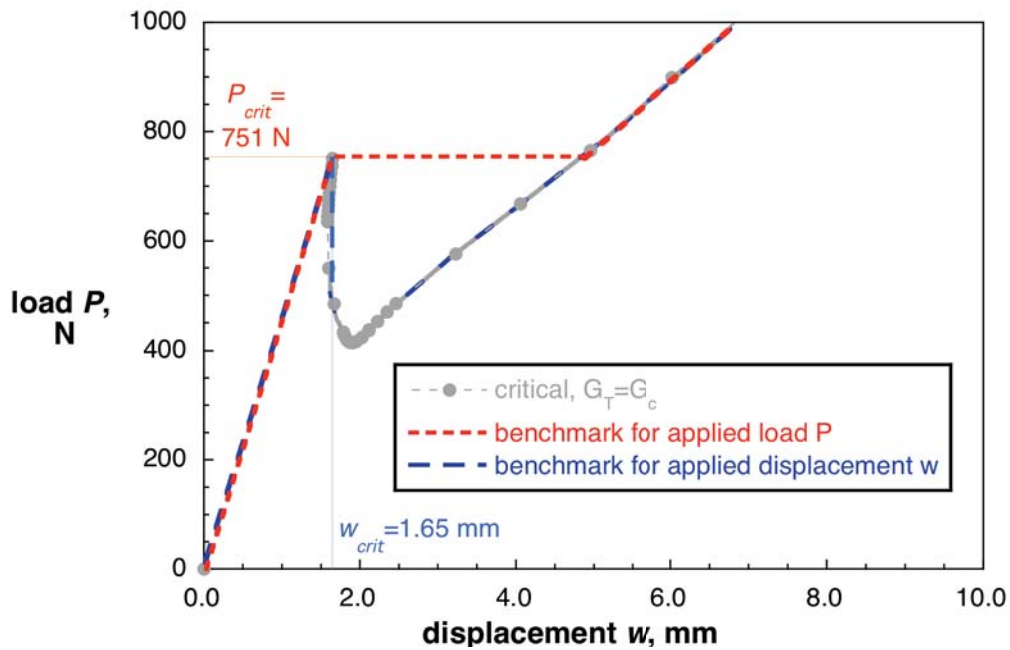


Figure 12. Calculated critical behavior and resulting benchmark cases for applied load, P , and displacement, w , for a MMB specimen (80% mode II).

Computed delamination propagation for applied displacement

The propagation analysis was performed in two steps using the model shown in Figure 5 starting from an initial delamination length, $a_0=25.4$ mm. In the first step, a displacement of $w=1.5$ mm was applied which nearly equaled the critical displacement, $w_{crit}=1.65$ mm, determined earlier. In the second step, the applied displacement was increased to $w=8.0$ mm. For this second step, automatic incrementation was used in Abaqus/Standard[®] and a small increment size (0.5% of the total step) was chosen at the beginning of the step. To reduce the risk of numerical instability and early termination of the analysis, a minimum allowed increment size (10^{-18} of the total step) was also chosen. The analysis was limited to 5000 increments.

Initially, analyses were performed using two-dimensional planar models (shown in Figure 5) without stabilization or viscous regularization. Using the default value $reltol=0.2$, the load and displacement exceeded the critical point and the analysis terminated (thick solid green line) as shown in Figure 13 where the computed resultant force (load P) is plotted versus the applied displacement w . By increasing the release tolerance to $reltol=0.5$, – as suggested by the Abaqus/Standard[®] error in the message (.msg) file – it was possible to extend the analysis without an error message until the load drop occurred and delamination propagation started as shown in Figure 13, (solid light blue line). However, the load drop occurred past the critical point and the analysis terminated soon afterwards due to convergence problems. The release tolerance was not increased any further as suggested in the Abaqus/Standard[®] error in the message (.msg) file. Previous analysis had shown that by increasing the release tolerance ($reltol>0.2$), termination of the analysis could be avoided, however, the results had not been in good agreement with the

benchmark [3,4]. Therefore, it was decided to introduce additional stabilization to obtain better agreement with the benchmark case.

The results computed when contact stabilization (cs) was added are plotted in Figure 14. A small stabilization factor ($cs=1 \times 10^{-6}$) was used for all cases since it had yielded good results in previous analyses [3, 4]. Initially, the release tolerance value was set at the default value ($reltol=0.2$) (dashed green line). For this parameter combination, the load increased past the critical point and delamination propagation started while the load dropped (dashed green line). The load/displacement path then ran parallel to the constant displacement branch of the benchmark result and later followed the stable propagation branch of the benchmark result.

To reduce the observed overshoot, the release tolerance was reduced. For a stabilization factor of $cs=1 \times 10^{-6}$ and release tolerance $reltol=0.1$ (solid blue line), the overshoot was reduced, and the computed load/displacement path then ran closer to the constant displacement branch of the benchmark result. However, just before reaching the minimum load, the displacement increased slightly followed by a small load drop. The results then followed the stable propagation branch of the benchmark result. Further reducing the release tolerance ($reltol=0.01$) yielded results that were in excellent agreement with the benchmark (dash-dotted red line). Due to the fine mesh, only a small saw-tooth pattern was observed along the stable path. In particular, good agreement could be achieved by selecting input parameters that had previously been determined during analyses of mode I DCB and mode II ENF specimens [3, 4].

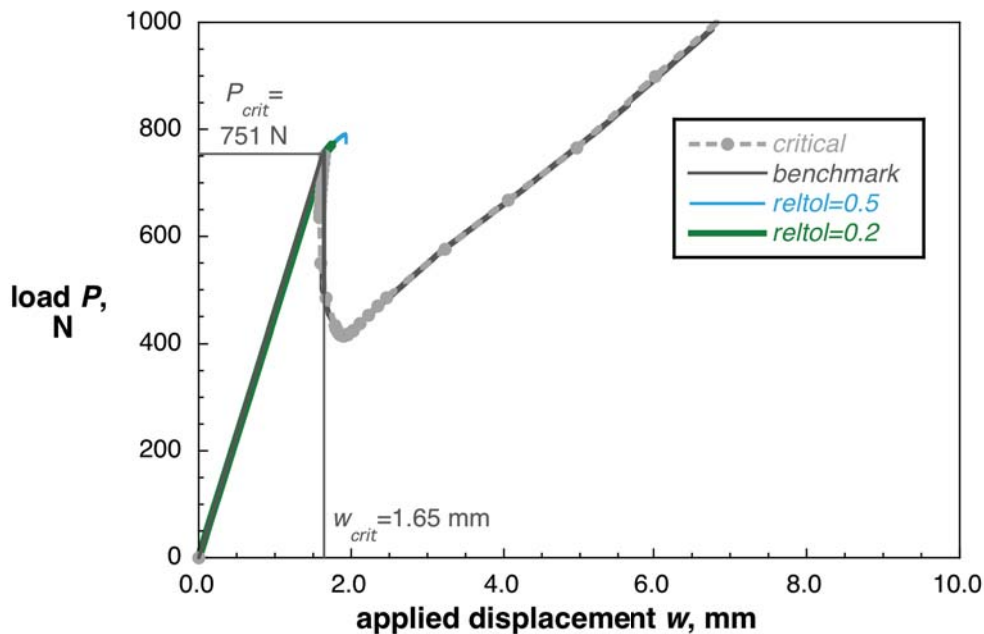


Figure 13. Computed critical load-displacement behavior for MMB specimen (80% mode II) obtained from 2D planar models (CPE4I) with different release tolerance settings.

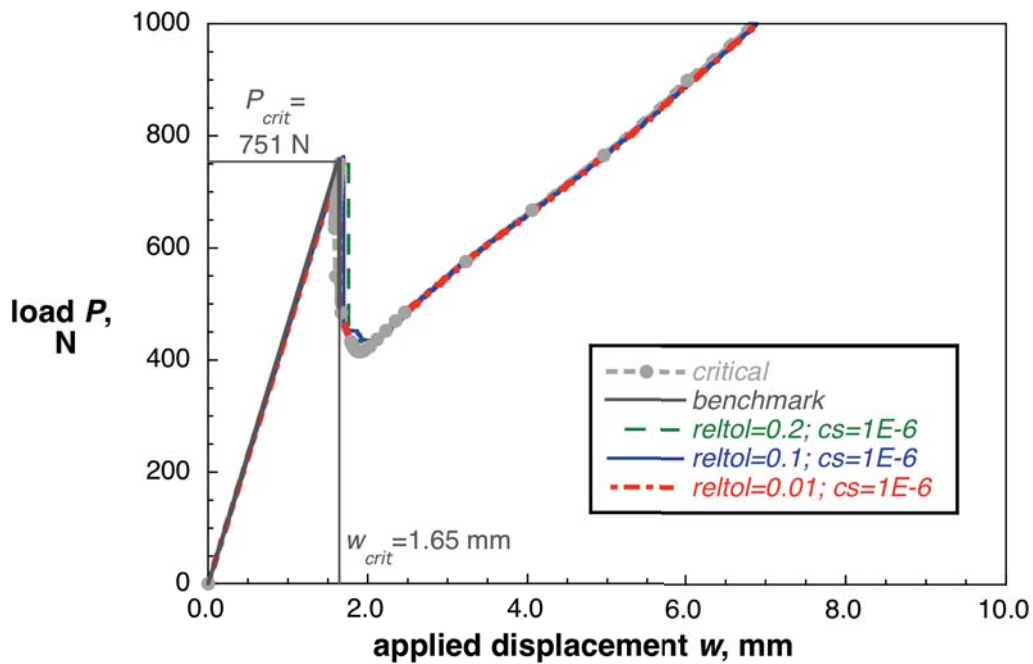


Figure 14. Computed critical load-displacement behavior for MMB specimen (80% mode II) obtained from 2D planar models (CPE4I) with added contact stabilization.

Computed delamination propagation for applied quasi-static load

The propagation analysis was performed in two steps using the model shown in Figure 5 starting from an initial delamination length, $a_0=25.4$ mm. In the first step, a load $P=730$ N was applied which equaled nearly the critical load, $P_{crit}=751$ N, determined earlier. In the second step, the total load was increased ($P=1000$ N). As before, automatic incrementation was used with a small increment size at the beginning (0.5% of the total step) and a very small minimum allowed increment (10^{-18} of the total step) to reduce the risk of numerical instability and early termination of the analysis. The analysis was limited to 5000 increments.

The same steps discussed in the section on applied displacement were followed. Initially, analyses were performed using two-dimensional planar models without stabilization or viscous regularization. Using the default value ($reltol=0.2$), the load increase stopped after reaching the critical point, but the analysis terminated immediately (thick solid green line) due to convergence problems, as shown in Figure 15. The release tolerance was not increased as suggested by the Abaqus/Standard[®] error in the message (.msg) file. Previous analysis had shown that by increasing the release tolerance ($reltol>0.2$), termination of the analysis could be avoided, however, the results had not been in good agreement with the benchmark [3,4]. Therefore, it was decided to introduce additional stabilization to obtain better agreement with the benchmark case.

The results computed when contact stabilization (cs) was added are plotted in Figure 16. A small stabilization factor ($cs=1 \times 10^{-6}$) was used for all cases since it had yielded good results in previous analyses [3, 4]. Initially, the release tolerance value was set at the default value ($reltol=0.2$) (dashed green line). For this parameter combination, the load increased up to the critical point and delamination

propagation started while the load remained constant (dashed green line). Also for the stable propagation path, the result was in good agreement with the benchmark result (solid grey line). Then, the release tolerance was reduced to $reltol=0.1$ (solid blue line) and further to $reltol=0.01$ (dash-dotted red line).

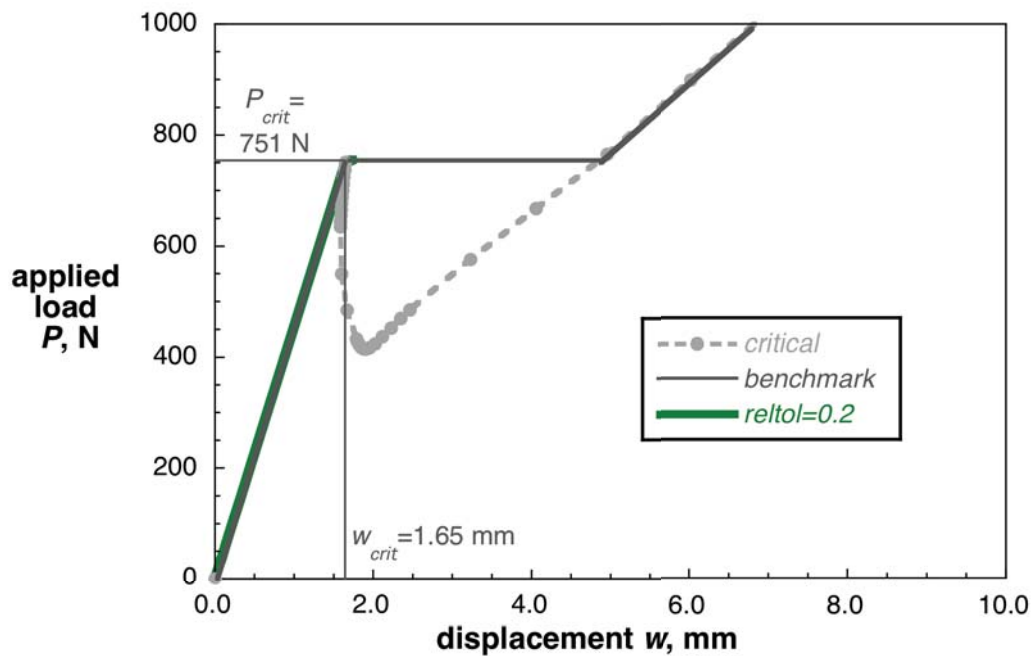


Figure 15. Computed critical load-displacement behavior for MMB specimen (80% mode II) obtained from 2D planar models (CPE4I) with different release tolerance settings.

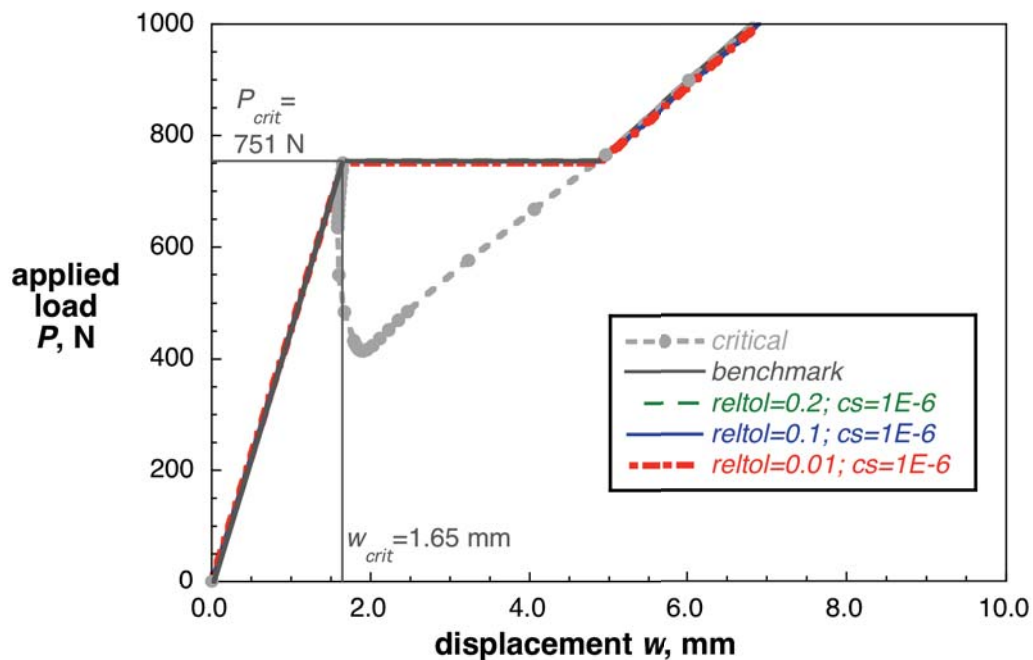


Figure 16. Computed critical load-displacement behavior for MMB specimen (80% mode II) obtained from 2D planar models (CPE4I) with added contact stabilization.

For all cases, the results were in good agreement with the benchmark results over the entire load/displacement range. In particular, good agreement could be achieved by selecting input parameters that had previously been determined during analyses of mode I DCB and mode II ENF specimens [3, 4].

SUMMARY AND CONCLUSIONS

The development and application of benchmark examples for the assessment of quasi-static delamination propagation capabilities was demonstrated for ANSYS[®] and Abaqus/Standard[®]. The examples selected were based on finite element models of Double Cantilever Beam (DCB), and Mixed-Mode Bending (MMB) specimens.

First, quasi-static benchmark results were created based on the approach developed in reference 3. Second, the delamination was allowed to propagate under quasi-static loading from its initial location using the automated procedure implemented in ANSYS[®] and Abaqus/Standard[®]. Input control parameters were varied to study the effect on the computed delamination propagation.

The results showed the following:

- The benchmarking procedure is independent of the analysis software.
- The benchmarking procedure was able to recreate the DCB benchmark case suggested by *NAFEMS*.
- The benchmarking procedure was capable of identifying the critical input parameters for a particular implementation and highlighting the differences in implementation.
- These input parameters are unique to the software studied and do not reflect real *physical* differences in delamination behavior.
- In general, good agreement between the results obtained from the propagation analysis and the benchmark results could be achieved by selecting the appropriate input parameters. However, selecting the appropriate input required an iterative procedure.
- For Abaqus/Standard[®] in particular, the results for automated delamination propagation analysis under quasi-static loading showed the following:
 - Using the default release tolerance ($reltol=0.2$) or increasing the value, as suggested in the user's manual, may help to overcome convergence problems, however, it leads to an undesired overshoot of the computed result compared to the benchmark.
 - A combination of release tolerance and contact stabilization is required to obtain more accurate results.
 - A gradual reduction of the release tolerance and contact stabilization over several analyses is suggested.
 - Good agreement between analysis results and the benchmarks could be achieved for release tolerance values ($reltol<0.1$) in combination with contact stabilization ($cs=1\times 10^{-6}$).
- For ANSYS[®], in particular, the results for automated delamination propagation analysis under static loading showed the following:
 - Automated analysis generally resulted in a converged solution, however, it led to undesired overshoot of the result.

- User input to control the time step for crack growth (*cgrow*) is required to obtain more accurate results, in particular for the propagation phase of the analysis. Repeatedly consistent results could be obtained when the initial time step, *dtime*, and the maximum allowable time step, *dtmax*, were equivalent and were equal to or smaller than 10^{-4} ($dtime=dtmax\leq 10^{-4}$).
- User input to control the automated time stepping (*autots*) is also required, in particular to capture the critical point of propagation onset or first node release. Repeatedly consistent results could be obtained when the initial time step, *dtimea*, and the maximum allowable time step, *dtmaxa*, were equivalent and were equal to or smaller than 10^{-3} ($dtimea=dtmaxa\leq 10^{-3}$).

Overall, the benchmarking procedure proved valuable by highlighting the issues associated with choosing the appropriate input parameters for the VCCT implementations in ANSYS[®] and Abaqus/Standard[®]. However, further assessment for mixed-mode delamination fatigue onset and growth is required. Additionally studies should include the assessment of the propagation capabilities in more complex specimens and on a structural level.

REFERENCES

- [1] E. F. Rybicki and M. F. Kanninen, "A Finite Element Calculation of Stress Intensity Factors by a Modified Crack Closure Integral," *Engineering. Fracture Mechanics*, Vol. 9, pp. 931-938, 1977.
- [2] R. Krueger, "Virtual Crack Closure Technique: History, Approach and Applications," *Applied Mechanics Reviews*, Vol. 57, pp. 109-143, 2004.
- [3] R. Krueger, "An Approach to Assess Delamination Propagation Simulation Capabilities in Commercial Finite Element Codes," NASA/TM-2008-215123, 2008.
- [4] R. Krueger, "Development and Application of Benchmark Examples for Mode II Static Delamination Propagation and Fatigue Growth Predictions," NASA/CR-2011-217305, NIA report no. 2011-02, 2011.
- [5] R. Krueger, "Development and Application of Benchmark Examples for Mixed-Mode I/II Quasi-Static Delamination Propagation Predictions," NASA/CR-2012-217562, NIA report no. 2012-01, 2012.
- [6] A. C. Orifici and R. Krueger, "Assessment of Static Delamination Propagation Capabilities in Commercial Finite Element Codes Using Benchmark Analysis," NASA/CR-2010-216709, NIA report no. 2010-03, 2010.
- [7] R. Krueger "Application of Benchmark Examples to Assess the Single and Mixed-Mode Static Delamination Propagation Capabilities in ANSYS," NASA/CR-2012-217588, NIA report no. 2012-04, 2012.
- [8] R. Krueger, "Development of a Benchmark Example for Delamination Fatigue Growth Prediction," NASA/CR-2010-216723, NIA report no. 2010-04, 2010.
- [9] G. A. O. Davies, "Benchmarks For Composite Delamination," Publication R00084: NAFEMS, 2002.
- [10] I. S. Raju and T. K. O'Brien, "Fracture Mechanics Concepts, Stress Fields, Strain Energy Release Rates, Delamination and Growth Criteria," in *Delamination Behavior of Composites*, S. Sridharan, Ed.: Woodhead Publishing in Materials, 2008.
- [11] M. L. Benzeggagh and M. Kenane, "Measurement of Mixed-Mode Delamination Fracture Toughness of Unidirectional Glass/Epoxy Composites with Mixed-Mode Bending Apparatus," *Composites Science and Technology*, Vol. 56, pp. 439-449, 1996.
- [12] *Abaqus Analysis User's Manual*, Abaqus/Standard[®], Version 6.10, DSS Simulia, 2010.
- [13] ANSYS, Inc. *Structural Analysis Guide*, 2010.
- [14] G. Lin, "VCCT and Crack Growth Simulation in ANSYS," presentation ANSYS, Inc., 2010.
- [15] D. Broek, *The Practical Use of Fracture Mechanics*: Kluwer Academic Publishers, 1991.